Article

Study of Effect of Secondary Cooling on Titanium Nitride Precipitation During Continuous Casting of High-strength Steel Slab

Sustainable Manufacturing and Foundry Practices
1(1) 80–87, 2026

DOI: 10.1177/IIF.261439608
Journal.indianfoundry.org
THE INSTITUTE OF INDIAN FOUNDRYMEN

Ajay Kumar Pradhan[1], Pabitra Palai[1], Pramod Yadav[1] and M Manjunathan[1]

Abstract

The special type of advanced high-strength steels (AHSS) based on nano precipitation strengthening mechanism was studied in the current work. It is a typical molybdenum and titanium based micro-alloyed steel under AHSS offers up to 800 Mpa tensile strength and have preferred application in the automobile industry owing to its impact on overall vehicle weight reduction with improved safety and fuel efficiency, The focus of study in this grade were failure due to cracking during forming on account of coarse Titanium Nitride (TiN) precipitate in such high-strength level above 800 Mpa tensile strength. The main challenges in this grade are chemical composition and casting parameters control, which have a direct influence on the microstructure and final properties that are attributed to precipitate size. The study has been done for the precipitation of TiN in high-strength steel by varying secondary cooling during slab casting. The model enabled the prediction of the expected inclusion size of TiN of a specific HS800 heats before rolling to enable slab decision. The main goal of this work was to obtain the dependence relationship between inclusion size and slab solidification and cooling rate during continuous casting.

Keywords

Chemical composition, high-strength steel, precipitation strengthening, continuous slab casting

[1]Steel Making Shop, TATA Steel Limited, Jajpur, Odisha, India

Corresponding author:
Ajay Kumar Pradhan, Steel Making Shop, TATA Steel Limited, Kalinganagar, Jajpur, Odisha 755026, India.
E-mail: ajay.pradhan3@tatasteel.com

Introduction

The growing demand from the automotive sector for lightweight vehicles, aimed at improving fuel efficiency and reducing greenhouse gas emissions, has driven steel manufacturers to develop advanced high-strength steels (AHSS). In response to this need, Steel makers have initiated the development of a high-strength steel grade with a minimum tensile strength of 800 MPa. The cleanliness of this steel is critical for determining product acceptance in automotive applications. This steel, along with other grades used in automotive underbody components such as suspension systems, cross members, and chassis, is produced through the conventional BOF–slab casting–hot rolling route. The HS800 grade is a micro-alloyed steel containing elements such as Nb, Ti, and Mo, along with an elevated manganese content as mentioned in Table 1. The grade initially reported a brittle failure at the customer end, specifically at the bent area of the components. It appears the cracks likely started near a hole in this bent region (as shown in Figure 1), potentially due to stress concentration exacerbated by a shorter distance between holes on the cracked side compared to crack-free areas. Microscopic examination revealed a notable presence of Titanium Nitride (TiN) inclusions, approximately 13–14 µm in size, both where cracks occurred and where the material remained intact. These inclusions are suspected to have played a role in the crack's propagation once it initiated from the stress point around the hole. The chemistry of the HS800 grade is attached.

Que et al. (2023) examined the distribution of TiN inclusions in the cross-section of a titanium micro-alloyed steel slab and found that the number density of these inclusions sharply decreases from the surface to the center, while their average size increases in the same direction. Higher cooling rates lead to greater undercooling, which results in finer TiN precipitation. Micrographs indicated that TiN inclusions are mainly cuboidal in shape with well-defined edges, as shown in Figure 2.

Yang et al. (2017) reviewed the precipitation of Ti(C,N) by the influence of austenite growth. Figure 3 shows the relationship between equilibrium

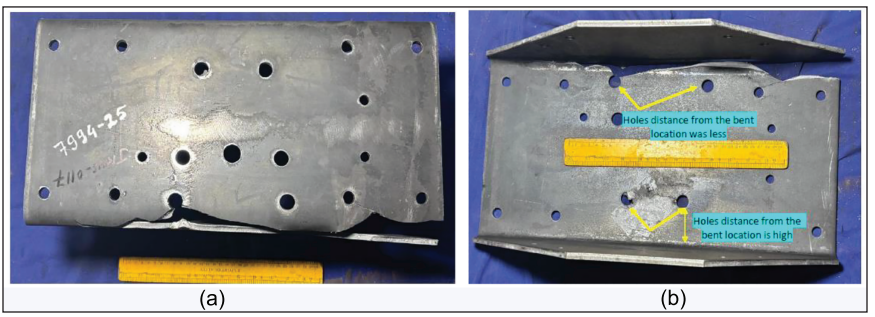

Figure 1. Failure Sample Indicating Cracks During Forming (a) Front View (b) Rear View.

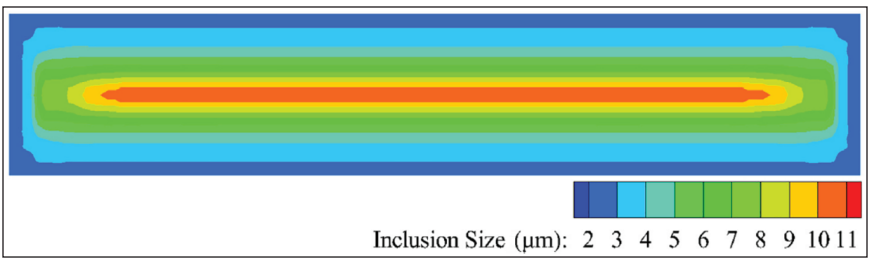

Figure 2. Size Distribution of TiN Inclusions in the Cross-sections.

Source: Que et al. (2023).

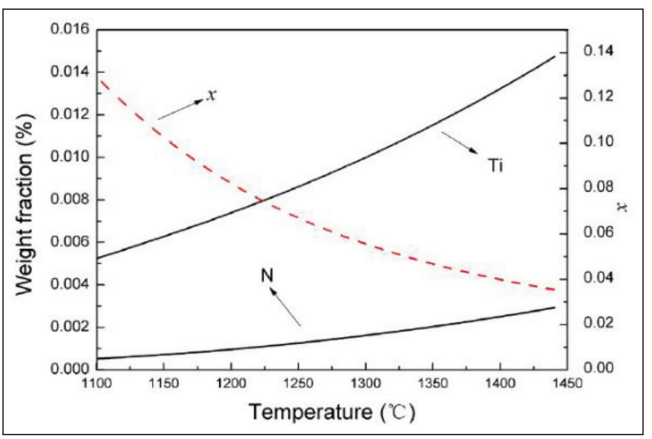

Figure 3. Equilibrium Concentration of Ti and N and Partition Coefficient *x* in Precipitates.

Source: Source: Yang et al. (2017).

concentration, the partition coefficient *x* of Ti(C*x*N1-*x*) precipitates, and temperature. As the temperature decreases, the equilibrium contents of Ti and N in austenite gradually decrease, while *x* gradually increases. The partition coefficient *x* is only about 0.04 when the temperature is between 1,350°C and 1,440°C, meaning the Ti(C*x*N1-*x*) precipitates at high temperatures are close to pure TiN. TiN possesses a lower equilibrium solubility than TiC; therefore, TiN demonstrates high stability in molten steel, austenite, and ferrite.

Yan et al. (2017) examined how TiN inclusions affect the tendency of low-carbon micro-alloyed steels to fracture under cleavage conditions. The role of TiN inclusions as potential crack initiation sites or pathways for crack propagation, influencing the material's toughness and overall mechanical performance. Nagata et al.'s (2002) paper explores how TiN forms in this slab-cast high-strength low-alloy steel. Specifically, it uses Transmission Electron Microscopy (TEM) to measure the size distribution of TiN particles and analyses how different cooling rates influence their precipitation.

Palai et al. (2013) precisely investigate how the constitutional segregation of alumina (Al_2O_3) in mold slag impacts the steel cleanliness during continuous slab

casting. The solid inclusion precipitates from the slag and infiltrates the steel, ultimately compromising its quality and impact on the final product. Won and Thomas (2001) proposed a simple multicomponent steel micro-segregation model by extending the Clyne-Kurz framework. This model predicts phase fraction and solidus temperature and indicates that cooling rate effects on spacing and solute distribution can offset each other, keeping solidus temperature stable.

However, the cleanliness of HS800 grade depends on the operational condition, that is, the steel-making and casting process parameter. The oversize inclusion clearly affects the behavior of the material at a different location. The casting process parameter, that is, secondary cooling, temperature, casting speed, etc., unusual variation can enhance the size of the inclusion. To find the inclusion size of TiN for current practice in the industry at the slab stage, and explore the different secondary cooling strategies at the continuous slab caster to mitigate the oversize inclusion of TiN.

Experimental

To understand the relation between precipitation size and cooling rate in continuous casting, an experimental study has been done. To study the microstructure at the slab stage with respect to variation of secondary cooling rate (Trial 1 & Trial 2) and different locations of slab as depicted in Figure 4b. Figure 4a represents the schematic diagram of a slab. The two planes, plane A and plane B, correspond to standard metallographic orientations used to study solidification structure in a continuously cast slab. Both planes are perpendicular to the casting direction (across the thickness and width of the slab). The purpose of both planes is to understand directional growth of dendrites/columnar grains along heat flow as well as solidification structure through thickness. It helps to identify defects like centerline segregation (CLS), porosity and internal cracks across the section. Different samples were taken from the inner arc (edge region) and center region, as depicted in Figure 4b.

To investigate the material, 150 mm-long sulfur print samples were first taken from the length of the prime slab. After these cooled, smaller 10 cm square sections were cut using a gas torch.

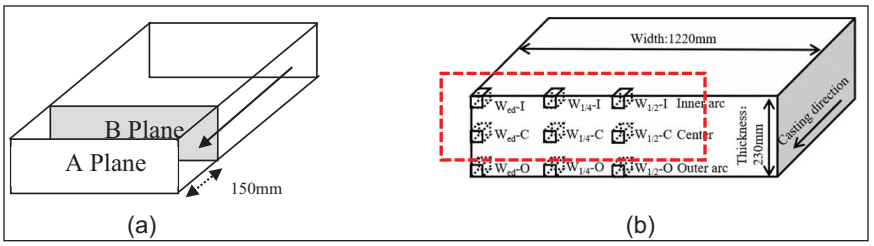

Figure 4. Diagram (a) Schematic Diagram of Slab (b) Schematic Diagram Slab Sample Location.

Table 1. Steel Chemistry of Cracked HS-800 Grade.

Element	C %	Mn %, Max	S %, Max	P %, Max	Al %	Ti %, Max	N (ppm), Max	Mo %
Range	0.05–0.07	1.7	0.005	0.014	0.04–0.06	0.12	70	0.24–0.27

Source: Chemistry ranges at plant.

Sampling was systematic:

- From the inner arc region: Three samples were collected—one from the edge (Wed-I), one from the quarter-width point (W1/4-I), and one from the center-width ($W_{1/2}$-I).
- From the center region: Another three samples were taken following the exact same width-wise pattern.

In total, 12 samples were prepared: 6 originating from the higher secondary cooling zone (Trial 1) and 6 from the lower secondary cooling zone (Trial 2). Following cutting, these samples underwent standard preparation procedures (like grinding and polishing) before their microstructures were analyzed in the metallography laboratory.

Results and Discussions

After sample cutting from the slab at different locations with respect to secondary cooling, the microstructure has been studied. It was found that the inclusion size of TiN is basically a cuboidal shape. Inclusion characterization was performed using energy dispersive spectroscopy (EDS), which confirmed that the observed precipitates are predominantly TiN, as indicated by the presence of strong Ti and N peaks along with minor Fe signals from the surrounding matrix. For statistical reliability, a total of 30 inclusions were measured at each sampling location (e.g., $W_1/_2$-C) under consistent imaging conditions. The average inclusion size and corresponding standard deviation were calculated using standard statistical methods as depicted in Figure 5. The results show that for Trial 1 (higher cooling rate), the average inclusion size is 4.0 ± 0.68 μm, whereas for Trial 2 (lower cooling rate), it is 4.8 ± 0.81 μm at the $W_{1/4}$-C location. The observed increase in inclusion size with increasing cooling rate is attributed to enhanced precipitation kinetics and limited solute diffusion during rapid solidification. The relatively moderate standard deviation values indicate a reasonably consistent size distribution, although some variation is expected due to local thermal and compositional heterogeneities.

It was also noted that higher cooling rates tend to produce a greater population of these precipitated TiN inclusions. This effect was observed in the comparison between Trial 1 and Trial 2 secondary cooling zones for the TiN inclusions.

As the cooling rate varies at different segments of the caster due to different water flow. Water level flow per unit time for Trial 1 and Trial 2 is depicted in Table 2. Casting speed of this grade is maintained between 0.9 and 1.1 mtr/min. The cooling rate for both Trial 1 and Trial 2 was calculated based on water flow.

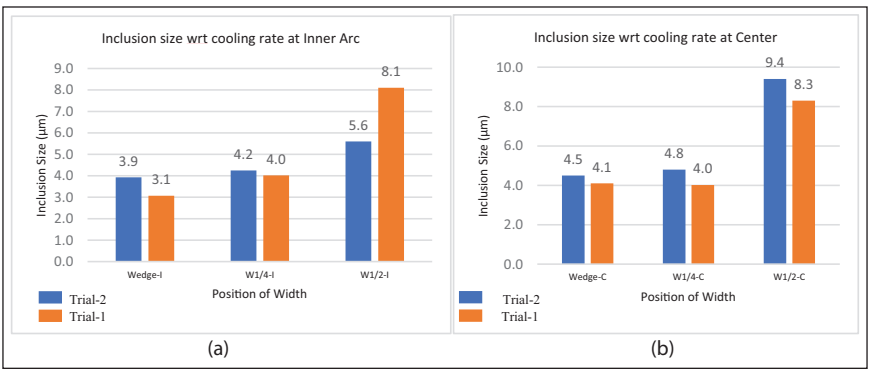

Figure 5. Size of a Precipitated Titanium Nitride (a) Inner Arc Region (b) Center Region.

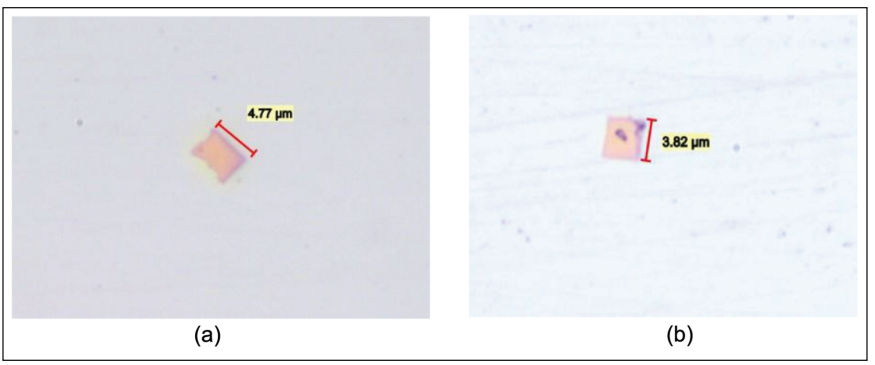

Figure 6. Inclusion Size of Precipitated TiN at the Same Location ($W_{1/2}$-C) in (a) Low Cooling Rate (b) High Cooling Rate.

Figure 5 represents the average inclusion size of precipitate TiN in variation location with varying of different of cooling rates (Trial 1 & Trial 2). In the Figure 5 orange and blue color represents the Trial 1 and Trial 2 respectively. In inner arc region, W_{edge}-I location average inclusion size finer for Trial 1 due to high cooling rate as compared to Trial 2. Whereas at the center location ($W_{1/2}$-I) the average size of precipitate TiN is coarser for Trial 2 due to low cooling rate.

The average inclusion size of precipitated TiN at center of width regions ($W_{1/2}$-C) in higher secondary cooling (Trial 1) and lower secondary cooling (Trial 2) is 8.3 ± 0.81 µm and 9.4 ± 0.89 µm, respectively.

The inclusion size of precipitated TiN in higher secondary cooling is more than in lower secondary cooling at the same location. The inclusion size of precipitated TiN at location ($W_{1/2}$-C) for Trial 2 and Trial 1 is 4.77µm and 3.82 µm, respectively, as depicted in Figure 6. This inclusion size is just for reference to understand the precipitate TiN shape and size.

Table 2. Cooling Profile of Both Trials.

Item	Trial 1 (Liter/Min)	Trial 2 (Liter/Min)
Spray ring nozzle	180–200	160–170
Narrow faces	35–40	30–32
Seg 1	160–190	140–150
Seg 2	100–120	80–100
Seg 3	300–330	220–250
Seg 4–5	180–200	130–150
Seg 6–7	160–190	130–150
Seg 8–9	70–100	50–70
Seg 10–12	140–150	140
Seg 13–16	150	150

Source: Cooling profile at plant.

Conclusion

Based on the systematic investigation involving composition control, continuous casting process parameters, secondary cooling effect, microstructural characterization, and reduction of the cracking effect of the typical AHSS steel strengthened with nano TiN precipitate, the main conclusions are summarized as follows. An experimental study on continuous slab casting of high manganese high-strength steel investigated, and the coarse precipitation of TiN inclusions was identified to cause cracking in the failed sample. By analyzing samples from various locations on the continuous casting slab, it was observed that increased secondary cooling rates lead to finer, more numerous TiN inclusions and these TiN inclusions were found to be cuboidal in shape. However, the highest average inclusion size has been found to be 9.4 ± 0.89 μm for center region of the slab at $W_{1/2}$-C owing to a slower rate of cooling practice at the slab caster. When nano-precipitates are subjected to high temperatures for longer times at slower cooling rates, they can coarsen and act as brittle phases. For instance, coarse TiN phases (>9 nm) on grain boundaries can trigger cleavage fracture rather than ductile deformation. In this study, a novel improved cooling rate practice has been successfully developed, resulting in cast steel with an excellent combination of strength and toughness. The formability and crack resistance significantly improved, offering a promising material solution for demanding applications in the automotive sector.

Declaration of Conflicting Interests

The authors declared no potential conflicts of interest with respect to the research, authorship, and/or publication of this article.

Funding

The authors received no financial support for the research, authorship, and/or publication of this article.

ORCID iD

Ajay Kumar Pradhan https://orcid.org/0009-0002-3021-1223

References

Nagata, M. T., Speer, J. G., & Matlock, D. K. (2002). Titanium nitride precipitation behavior in thin-slab cast high-strength low-alloy steels. *Metallurgical and Materials Transactions A*, *33*(10), 3099–3110. https://doi.org/10.1007/s11661-002-0294-z

Palai, P., Sahoo, P., Dey, A., Roy, T. K., & Mahashabde, V. (2013). Constitutional segregation of Al_2O_3 in slag and its impact on steel cleanliness during continuous casting. *Metallurgical and Materials Transactions B*, *44*(5), 1185.

Que, G., Song, S., Nyembwe, A., Xue, Z., Qi, J., & Deng, Z. (2023). TiN inclusions distribution in the composite cross section of titanium micro-alloyed steel slab: Thermochemical modeling and automatic statistic analysis. *Journal of Materials Research and Technology*, *26*, 5383–5392. https://doi.org/10.1016/j.jmrt.2023.08.247

Won, Y. M., & Thomas, B. G. (2001). Simple model of micro segregation during solidification of steels. *Metallurgical and Materials Transactions A*, *32*(7), 1755–1767.

Yan, W., Shan, Y., & Yang, K. (2007). Influence of TiN inclusions on the cleavage fracture behaviour of low-carbon micro alloyed steels. *Metallurgical and Materials Transactions A*, *38*(6), 1211–1222.

Yang, L., Li, Y., Xue, Z. L., & Cheng, C. G. (2017). Influence of Ti(C,N) precipitates on austenite growth of micro-alloyed steel during continuous casting. *China Foundry*, *14*(5), 421–428. https://doi.org/10.1007/s41230-017-7098-7